

Flexibility in Anaerobic Metabolism as Revealed in a Mutant of *Chlamydomonas reinhardtii* Lacking Hydrogenase Activity^{*§}

Received for publication, May 21, 2008, and in revised form, December 29, 2008 Published, JBC Papers in Press, December 31, 2008, DOI 10.1074/jbc.M803917200

Alexandra Dubini^{‡§}, Florence Mus[¶], Michael Seibert[§], Arthur R. Grossman[¶], and Matthew C. Posewitz^{§||1}

From the [‡]Environmental Science and Engineering Division, Colorado School of Mines, Golden, Colorado 80401, the [§]National Renewable Energy Laboratory, Golden, Colorado 80401, the [¶]Department of Plant Biology, Carnegie Institution, Stanford, California 94305, and the ^{||}Department of Chemistry and Geochemistry, Colorado School of Mines, Golden, Colorado 80401

The green alga *Chlamydomonas reinhardtii* has a network of fermentation pathways that become active when cells acclimate to anoxia. Hydrogenase activity is an important component of this metabolism, and we have compared metabolic and regulatory responses that accompany anaerobiosis in wild-type *C. reinhardtii* cells and a null mutant strain for the *HYDEF* gene (*hydEF-1* mutant), which encodes an [FeFe] hydrogenase maturation protein. This mutant has no hydrogenase activity and exhibits elevated accumulation of succinate and diminished production of CO₂ relative to the parental strain during dark, anaerobic metabolism. In the absence of hydrogenase activity, increased succinate accumulation suggests that the cells activate alternative pathways for pyruvate metabolism, which contribute to NAD(P)H reoxidation, and continued glycolysis and fermentation in the absence of O₂. Fermentative succinate production potentially proceeds via the formation of malate, and increases in the abundance of mRNAs encoding two malate-forming enzymes, pyruvate carboxylase and malic enzyme, are observed in the mutant relative to the parental strain following transfer of cells from oxic to anoxic conditions. Although *C. reinhardtii* has a single gene encoding pyruvate carboxylase, it has six genes encoding putative malic enzymes. Only one of the malic enzyme genes, *MME4*, shows a dramatic increase in expression (mRNA abundance) in the *hydEF-1* mutant during anaerobiosis. Furthermore, there are marked increases in transcripts encoding fumarase and fumarate reductase, enzymes putatively required to convert malate to succinate. These results illustrate the marked metabolic flexibility of *C. reinhardtii* and contribute to the development of an informed model of anaerobic metabolism in this and potentially other algae.

Chlamydomonas reinhardtii is a unicellular, soil-dwelling, photosynthetic green alga that has a diversity of fermentation pathways, inferred from the full genome sequence (1, 2). It uses

these pathways for ATP production during anoxia, catabolizing starch and other intracellular carbon substrates into the predominant fermentation products formate, acetate, ethanol, CO₂, and molecular hydrogen (H₂) in what is classified as heterofermentation (2–7). These metabolic pathways would be active primarily at night when high rates of respiration and the absence of photosynthetic O₂ evolution cause the rapid establishment of anoxia (8), especially in soil environments with high concentrations of microbes. Moreover, *C. reinhardtii* can balance the use of the tricarboxylic acid cycle with fermentation when the rate of respiratory O₂ consumption exceeds the rate of photosynthetic O₂ evolution (3, 4, 9). The catabolism of intracellular carbon stores during anoxic acclimation is a key component of *C. reinhardtii* metabolism as this alga does not appear to effectively assimilate extracellular sugars. Acquiring a better understanding of cellular metabolisms in algae such as *C. reinhardtii* under various conditions will facilitate the development of physiological models that predict metabolic circuits and the interactions among these circuits. Additionally, the secretion of fermentative metabolites by *C. reinhardtii* (and other algae) likely has significant impacts on the population dynamics of microbial consortia in environments inhabited by *C. reinhardtii*. There is also the potential to leverage the unique metabolic flexibility of *C. reinhardtii* for the production of valuable metabolites such as H₂, organic acids, and ethanol as renewable bioenergy carriers (4, 10, 11).

Although studies of *C. reinhardtii* metabolism have already significantly advanced our understanding of cellular responses to anoxia (5–7, 12), additional research efforts are required to gain further insights into the proteins involved in adaptation and acclimation of the cells to anaerobiosis, the modulation of cellular metabolite levels under these conditions, and the accurate localization of fermentation pathways and proteins to specific subcellular compartments. The availability of the *C. reinhardtii* genome sequence, combined with high throughput “omics”-based approaches, will be critical in this effort. Moreover, the use of specific mutant strains can help establish the foundation for a more comprehensive understanding of how cells adjust metabolite fluxes when specific reactions are blocked.

A number of studies have demonstrated that *C. reinhardtii* can rapidly acclimate to anaerobiosis by shifting to fermentative metabolisms (5–7, 12–14). The catabolism of pyruvate to acetyl-CoA in *C. reinhardtii* may proceed via fermentation pathways that use either PFL1 (pyruvate formate-lyase) (5, 6, 12, 15) or PFR1 (pyruvate ferredoxin oxidoreductase) (5, 6, 12).

* This work was supported by the Office of Biological and Environmental Research, GTL Program, Office of Science, United States Department of Energy (to A. R. G., M. C. P., and M. S.), by National Science Foundation Grant MCB 0235878 (to A. R. G.), and by Air Force Office of Scientific Research Grant FA9550-05-1-0365 (to M. C. P.). The costs of publication of this article were defrayed in part by the payment of page charges. This article must therefore be hereby marked “advertisement” in accordance with 18 U.S.C. Section 1734 solely to indicate this fact.

§ The on-line version of this article (available at <http://www.jbc.org>) contains supplemental Tables I and II and Fig. 1.

¹ To whom correspondence should be addressed. Tel.: 303-384-6350; Fax: 303-384-6150; E-mail: matthew_posewitz@nrel.gov or mposewit@mines.edu.

Flexibility in Anaerobic Metabolism

The acetyl-CoA is further metabolized to ethanol and/or acetate, and the reduced ferredoxin generated by PFR1 activity is putatively oxidized by a number of redox proteins, including one or both of the two *C. reinhardtii* [FeFe] hydrogenases (HYDA1 and HYDA2) (16, 17), which are localized to the chloroplast stroma (18, 19). A recently isolated *C. reinhardtii* mutant, *hydEF-1*, is devoid of hydrogenase activity (20, 21) because of disruption of an [FeFe] hydrogenase maturase, which is required for proper enzyme assembly (20–24); consequently, neither of the hydrogenases are active in the mutant strain.

In this study we use molecular and physiological approaches to examine dark, anoxic acclimation of the *C. reinhardtii* *hydEF-1* mutant. Interestingly, the mutant secretes much higher levels of succinate during anoxia than the parental strain. Furthermore, transcripts encoding PYC1 (pyruvate carboxylase) and MME4 (a malic enzyme) increase significantly in the mutant relative to the parental strain during anaerobiosis. Both of these proteins have the ability to carboxylate pyruvate, providing precursors for the fermentative production of succinate. Additionally, transcripts encoding fumarase (FUM1 and FUM2) and FMR1 (fumarate reductase), enzymes that catalyze the final steps of succinate synthesis, are elevated in the *hydEF-1* strain. Utilization of these pathways for succinate synthesis would result in NADH reoxidation, which would sustain additional cycles of glycolysis and explain both the relative increase in succinate and decrease in CO₂ production during anaerobiosis in the mutant relative to the parental strain. Microarray studies were also performed and reveal that several transcripts encoding proteins associated with cellular redox functions and other aspects of anaerobic metabolism are differentially regulated in the mutant relative to the parental strain. These findings are discussed with respect to the identification of potential new fermentation pathways and the flexibility of whole-cell metabolism in *C. reinhardtii* under dynamic environmental conditions.

EXPERIMENTAL PROCEDURES

Strains and Growth Conditions—*C. reinhardtii* CC-425 (*cw15, sr-u-60, arg7-8, mt⁺*) and *hydEF-1* mutant (derived from CC-425) cells were grown in Tris/acetate/phosphate medium (TAP)² (pH 7.2), supplemented with 200 mg·liter⁻¹ arginine for CC-425. Algal cultures were maintained at 25 °C, vigorously bubbled with air enriched with 3% CO₂, stirred using a magnetic stir bar, and illuminated with continuous light of 80 μmol photon m⁻² s⁻¹ photosynthetically active radiation at the surface of 1-liter Roux culture bottles (255 × 55 × 120 mm), in which cell densities ranged from 1 × 10⁵ to 3 × 10⁶ cells/ml of culture.

Chlorophyll Measurements—Chlorophyll *a* and *b* content were determined spectrophotometrically in 95% ethanol (25).

Anaerobic Induction of Liquid Cell Suspensions—*C. reinhardtii* cultures were grown on TAP medium to ~16–24 μg·ml⁻¹ total chlorophyll, centrifuged (500 ml of cells) at 3,000 × *g* for 1 min, and the cell pellet resuspended in one-tenth volume (50 ml) of anaerobic induction buffer containing 50 mM potassium phosphate (pH 7.2) and 3 mM MgCl₂ (26). The cells were then transferred to a sealed anaerobic vial in the dark and flushed with argon for 30 min. For measuring H₂ and O₂ production rates, 200 μl of cell cultures were placed in a Clark-type oxygen electrode assay chamber as described previously (6, 20). Clark-type oxygen electrodes were used simultaneously to measure light-induced H₂ and O₂ production rates. To measure fermentative H₂ production, 400 μl of head space gas was withdrawn from the sealed anaerobic vials and analyzed by gas chromatography (Hewlett Packard 5890 series II) using a Supelco column (60/80 mol sieve 5A 6 feet × 1/8 inch) coupled to a TCD detector. H₂ remaining in solution was quantified using the Clark-type oxygen electrode described above without illumination of the sample chamber.

CO₂ Measurement—CO₂ levels were below detection limits in the serum vial head space of anaerobically acclimated cells. Therefore, following anaerobic induction, 1 ml of anoxic cells was transferred in a gas-tight syringe to a sealed vial into which 1 ml of 1 M HCl was added. The acidified cell suspension was vigorously shaken to liberate CO₂, which was quantified by gas chromatography (Hewlett Packard 5890 series II) using a Supelco column (80/100 PORAPAK N 6 feet × 1/8 inch × 2.1 mm) coupled to a TCD detector.

Metabolite Analysis—Organic acid analysis was performed by liquid chromatography (Hewlett Packard Series 1050 HPLC) using an Aminex HPX-87H (300 × 7.8 mm) ion exchange column. Dark-adapted cells were collected at the indicated time points and centrifuged (10,000 × *g* for 1 min), and the supernatant was transferred to a new vial and frozen in liquid N₂ for subsequent analysis. Samples were thawed, centrifuged, and filtered prior to HPLC analysis. One hundred μl of cell culture supernatant was injected onto the column and eluted using 8 mM filtered sulfuric acid (J. T. Baker, Inc.) as the mobile phase at a flow rate of 0.5 ml·min⁻¹ at 45 °C. Retention peaks were recorded using Agilent ChemStation software, and quantifications were performed by comparisons with known amounts of standard for each of the organic acids.

Ethanol was measured using a YSI 2700 SELECT electrochemical probe (YSI Inc., Yellow Springs, OH). Identical supernatants were used for metabolite and ethanol analysis; 10 μl of the supernatant was required for ethanol analysis.

Extraction of RNA—Total RNA was isolated using the Plant RNA reagent, as described by the manufacturer (Invitrogen). Approximately 40 μg of isolated RNA was treated with 5 units of RNase-free DNase (Ambion, Austin, TX) for 30 min at room temperature. The Qiagen RNeasy MinElute kit (Qiagen, Valencia, CA) was used to purify total RNA. The A₂₆₀ of the eluted RNA was measured, and 4 μg of purified RNA was reserved to prepare labeled samples for microarray analysis.

Reverse Transcriptase Real Time PCR (qPCR)—The abundance of specific transcripts in total mRNA from each sample was quantified by reverse transcriptase real time PCR, designated qPCR, using the Engine Opticon system (Bio-Rad). First

² The abbreviations used are: TAP, Tris/acetate/phosphate medium; qPCR, quantified by reverse transcriptase real time PCR; HPLC, high pressure liquid chromatography; PEP, phosphoenolpyruvate; PEPC, phosphoenolpyruvate carboxylase; PCK, phosphoenolpyruvate carboxylase; MDH, malate dehydrogenase; FUM, fumarase; FMR, fumarate reductase; MME, malic enzyme.

strand cDNA synthesis was primed on purified total RNA using specific primers for each *C. reinhardtii* gene of interest. The specific primers (at 0.5 μM each; supplied by IDT) were annealed to 250 ng of DNA-free total RNA and extended for 1 h at 55 °C using 200 units of the reverse transcriptase Superscript III (Invitrogen). Four μl of the single-stranded cDNA from the reverse transcriptase reaction (final volume, 20 μl) was used as the template for real time PCR amplifications, which were performed using the DyNAmo HS SYBR green reverse transcription-PCR kit according to the manufacturer's instructions (Finnzymes, Woburn, MA). Specific primers (0.3 μM) used for amplification were designed to generate amplicons of 100–200 nucleotides. Amplifications were performed using a Bio-Rad iCycler iQ detection system and the following cycling parameters: an initial single step at 95 °C for 10 min (denaturation) followed by 40 cycles of (a) 94 °C for 30 s (denaturation), (b) 56 °C for 45 s (annealing), and (c) 72 °C for 30 s (elongation). Following the 40 cycles, a final elongation/termination step was performed at 72 °C for 10 min. Primers used for qPCR are shown in supplemental Table 1, and were designed using Primer3 software (available on line). The relative expression ratio of a target gene was calculated based on the $2^{-\Delta\Delta C_T}$ method (27), using the average cycle threshold (C_T) calculated from triplicate measurements. Relative expression ratios from three independent experiments (different experimental replicates) are reported. The level of accumulation of the *RACK1* transcript was used as a normalization control because it shows near constant expression under the conditions used in these experiments.

Microarray Fabrication—Microarrays were fabricated at the Stanford Functional Genomics Facility at Stanford University, as described previously (6).

Labeling and Purification of Reverse-transcribed cDNAs—Labeling and purification of reverse-transcribed cDNAs were performed as described previously (28). Briefly, 4 μg of purified RNA was adjusted to 4 μl with sterile MilliQ-treated water. One μl of oligo(dT)-(V) (2 $\mu\text{g}\cdot\mu\text{l}^{-1}$) was heated for 10 min at 70 °C and quickly chilled on ice. The following reagents were added sequentially to the reaction mixture: 2 μl of 5 \times superscript buffer; 1 μl of 0.1 M dithiothreitol; 0.2 μl of 50 \times dNTPs (5 mM dATP, dCTP, and dGTP and 10 mM dTTP); 1 μl of Cy3- or Cy5-dUTP; and 0.8 μl of Superscript III (200 units $\cdot\mu\text{l}^{-1}$). The final reaction volume was 10 μl . After allowing the reaction to proceed at 42 °C for 2 h, an additional aliquot of 0.5 μl of Superscript III was added, and the reaction was continued for an additional 1 h at 50 °C. The reaction was stopped by the addition of 0.5 μl of 500 mM EDTA and 0.5 μl of 500 mM NaOH, and the solution was incubated at 70 °C for 10 min. Neutralization of the reaction mixture was achieved by adding 0.5 μl of 500 mM HCl. The QIAquick PCR purification kit (Qiagen, Valencia, CA) was used to purify the labeled cDNA as described previously (6).

Hybridization to the Oligonucleotide Array—Pre-hybridization and hybridization of fluorescent-labeled probes and washing of the arrays were as described previously (6, 28). Detailed and updated versions of the protocols used for RNA labeling, slide pre-hybridization, hybridization, and washing can be downloaded from the Chlamydomonas Center website.

TABLE 1

Concentrations of fermentation products secreted by the *Chlamydomonas hydEF-1* mutant and the parental strain, CC-425, following exposure to dark anaerobiosis at the indicated times

Cells were purged for 30 min with argon in the dark and then maintained in the dark for up to 24 h. Samples were taken at 0.5, 2, 4, and 24 h, centrifuged, and filtered, and the medium was analyzed for succinic acid, ethanol, acetic acid, and formic acid using HPLC. CO_2 is reported as the change in CO_2 concentration relative to the concentration at the start of the anaerobic induction. H_2 and CO_2 accumulations were analyzed as described under "Experimental Procedures." Data are from three independent experiments.

| Time | Fermentation products | | | | | |
|----------------|-----------------------|-----------------|---------------|-----------------|---------------|---------------|
| | CO_2 | H_2 | Formic acid | Succinic acid | Acetic acid | Ethanol |
| <i>h</i> | <i>mmol/liter</i> | | | | | |
| CC-425 | | | | | | |
| 0.5 | -0.05 \pm 0.09 | 0.02 \pm 0.01 | 0.5 \pm 0.2 | BD ^a | 0.9 \pm 0.2 | 0.2 \pm 0.1 |
| 2 | 0.14 \pm 0.02 | 0.03 \pm 0.01 | 1.3 \pm 0.1 | 0.1 \pm 0.1 | 1.5 \pm 0.1 | 0.7 \pm 0.1 |
| 4 | 0.64 \pm 0.08 | 0.06 \pm 0.01 | 2.2 \pm 0.1 | 0.1 \pm 0.1 | 1.8 \pm 0.3 | 1.1 \pm 0.2 |
| 24 | ND ^b | ND | 4.8 \pm 0.2 | 0.1 \pm 0.1 | 4.3 \pm 0.3 | 1.9 \pm 0.1 |
| hydEF-1 | | | | | | |
| 0.5 | -0.09 \pm 0.01 | BD | 0.3 \pm 0.2 | 0.1 \pm 0.03 | 0.4 \pm 0.2 | BD |
| 2 | -0.09 \pm 0.02 | BD | 1.0 \pm 0.1 | 0.2 \pm 0.1 | 0.7 \pm 0.2 | 0.4 \pm 0.1 |
| 4 | -0.03 \pm 0.01 | BD | 1.5 \pm 0.1 | 0.4 \pm 0.2 | 1.0 \pm 0.2 | 0.7 \pm 0.1 |
| 24 | ND | ND | 3.5 \pm 0.2 | 1.2 \pm 0.1 | 2.0 \pm 0.2 | 0.8 \pm 0.2 |

^a BD means below detection.

^b ND means not determined.

Scanning, Quantification, and Analysis of the Slides—Microarray slides were scanned for Cy5 and Cy3 fluorescent signals using a GenePix 4000B scanner (Molecular Devices) as described previously (6). Spot positions were defined using SpotReader (Niles Scientific). Analyses of the data were performed using GeneSpring 6.1 (Agilent Technologies, Foster City, CA). Images of the fluorescence at 532 nm for Cy3 and 635 nm for Cy5 were recorded and analyzed from the complete array sets (three experimental replicates for the time point 0.5 h, four experimental replicates for the time points 2 and 4 h, and three slides per time point for each experimental replicate, with two copies of each cDNA per slide). Error models were computed based on replicates. Signal ratios were considered to meet threshold criteria if they passed Student's *t* test for significance with a *p* value of ≤ 0.05 .

RESULTS

Metabolite Analyses—The *C. reinhardtii* *hydEF-1* mutant lacks hydrogenase activity because of disruption of the *HYDEF* gene, which encodes a hydrogenase maturase (20). This mutant was used to investigate the physiological responses of *C. reinhardtii* in the absence of H_2 metabolism during anaerobic acclimation. The fermentative products that accumulated in the medium during anoxia in both cultures mutant and parental control are shown in Table 1. Four significant differences observed between mutant and parental cells were as follows: (a) the absence of H_2 production in the mutant relative to the parental strain; (b) a marked difference in accumulation of CO_2 between the two strains; (c) a slight reduction in the rate of accumulation of formate, acetate, and ethanol in the mutant relative to the parental strain; and (d) elevated production of succinate, only in the mutant. Rescue of the *hydEF-1* mutant phenotype and restoration of the fermentation profile (along with H_2 and CO_2 production) observed in the parental strain was achieved by introduction of a functional copy of the *HYDEF* gene (data not shown). The complemented strain was not used as a reference in the microarray experiments as integration of

Flexibility in Anaerobic Metabolism

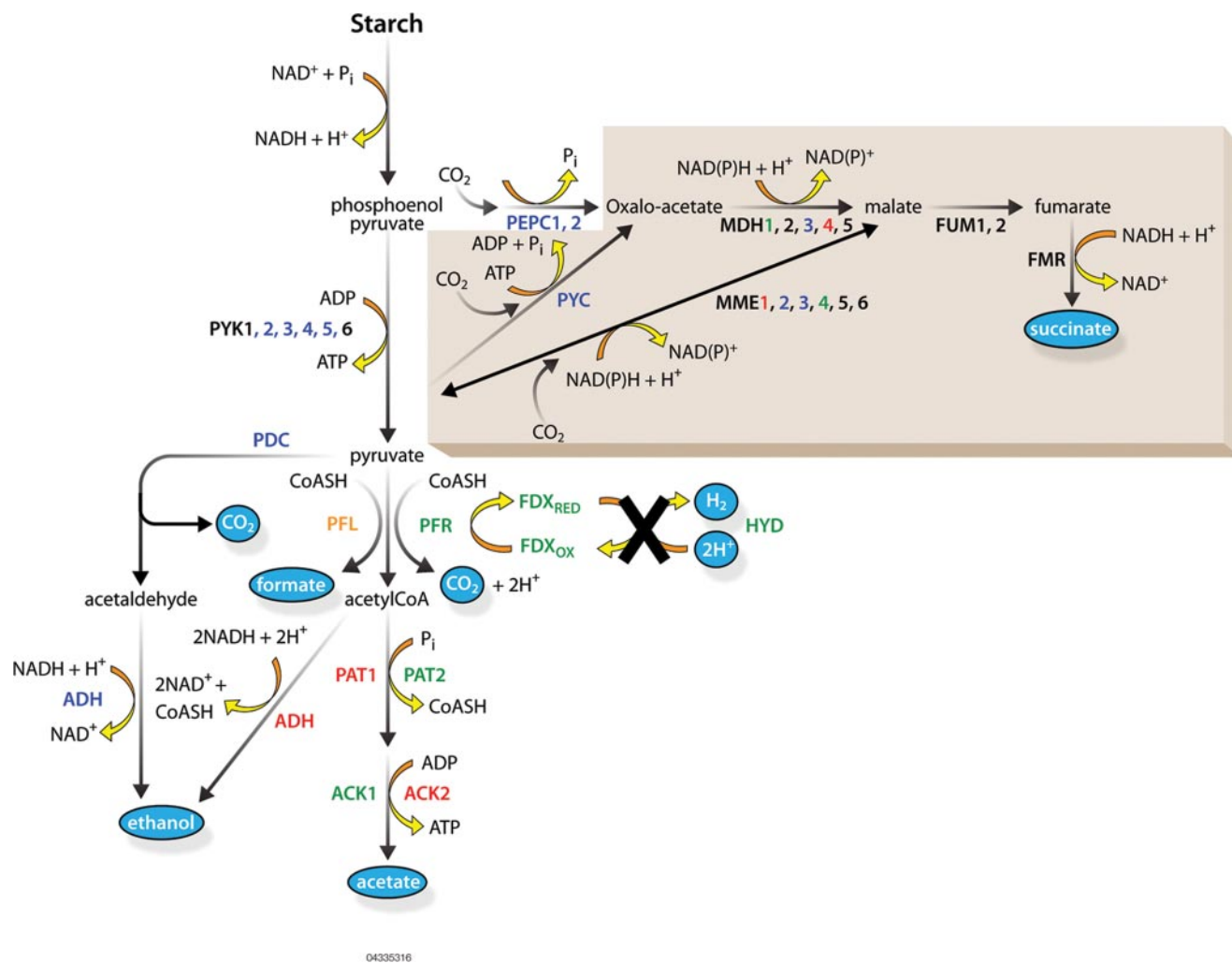


FIGURE 1. **Anaerobic metabolic pathways in *C. reinhardtii*.** Pathways at the upper right are proposed for succinate production and NADH reoxidation in the *hydEF-1* mutant. Proteins encoded in the *C. reinhardtii* genome that are associated with the metabolisms depicted include the following: *ACK*, acetate kinase; *ADH*, bifunctional acetaldehyde/alcohol dehydrogenase (alcohol dehydrogenase only in the case of the PDC pathway); *FDX*, ferredoxin; *FMR*, fumarate reductase; *FUM*, fumarase; *HYD*, hydrogenase; *MDH*, malate dehydrogenase; *MME*, malic enzyme; *PAT*, phosphate acetyltransferase; *PDC*, pyruvate decarboxylase; *PEPC*, phosphoenolpyruvate carboxylase; *PFL*, pyruvate formate-lyase; *PFR*, pyruvate-ferredoxin oxidoreductase; *PYC*, pyruvate carboxylase; *PYK*, pyruvate kinase. Known or putative cellular localizations of the proteins depicted are coded by color as follows: green for the chloroplast, red for the mitochondrion, orange for dual chloroplast/mitochondrion localization, blue for cytoplasm, and black for unknown. The cellular localizations of MDH1, -3, and -4, ACK2, PFL, and PAT1 were experimentally determined by Allmer *et al.* (46) and Atteia *et al.* (5), respectively. The cellular localizations of the other enzymes were determined using ChloroP, TargetP, and Predotar softwares and are highly speculative. When possible a final predicted localization was determined by doing an average of all predictions.

the introduced *HYDEF* gene into the genome could disrupt another cellular function.

Succinate is not detected in significant amounts in the medium of the parental culture but does accumulate in the mutant culture, particularly after longer periods (4 and 24 h) of anaerobiosis. CO₂ levels do not increase significantly during acclimation to anaerobiosis in the mutant, whereas in parental cells CO₂ levels steadily rise over the acclimation period. To account for succinate production and the near constant CO₂ level in the mutant, we identified genes on the draft genome encoding enzymes associated with fermentative succinate production. These encoded enzymes were placed into metabolic pathways (Fig. 1) leading to the fermentative production of succinate, which requires the carboxylation of a three-carbon substrate and is consistent with diminished CO₂ accumulation in the mutant relative to the parental strain. The proteins associated with the succinate pathways depicted in Fig. 1 are given in

Table 2. Because hydrogenase activity is absent in the mutant, pyruvate flux via the pyruvate ferredoxin oxidoreductase (PFR1) pathway is anticipated to be altered because hydrogenase can no longer participate in PFR1/ferredoxin reoxidation. However, it should be noted that additional metabolic pathways could potentially oxidize ferredoxin, such as sulfite reductases or NAD(P)H-ferredoxin oxidoreductases, and metabolic flux could still proceed via PFR1 provided ferredoxin was reoxidized by alternative pathways. Under our experimental conditions the parental strain accumulates 10-fold more CO₂ than H₂ (on a molar basis) indicating that other pathways are involved in the process under our experimental conditions (Table 1). If all of the reduced ferredoxin was oxidized by hydrogenase, this stoichiometry (CO₂/H₂) should be 1:1. Relative to the parental strain, the increased succinate accumulation observed in the mutant would consume both the reducing equivalents and nearly all of the CO₂ generated by pyruvate

TABLE 2

***Chlamydomonas* proteins associated with anoxic metabolism and succinate production in the *hydEF-1* mutant**

The sequences of the proteins are based on gene models from version 3.0 of the genome sequence. Both protein IDs and associated annotation provided on the JGI Browser are given.

| Enzyme assigned name | Annotation | Protein ID |
|--|---|------------------------|
| FUM1 | Fumarase | 195953 |
| FUM2 | Fumarase | 196655 |
| Fumarate reductase | Fumarate reductase/succinate dehydrogenase flavoprotein | 145357 |
| MDH1 NAD-dependent | Lactate/malate, dehydrogenase | 137163 |
| MDH2 NAD-dependent | Malate dehydrogenase | 126023 |
| MDH3 NAD-dependent | Malate dehydrogenase | 158129 |
| MDH4 NAD-dependent | Malate dehydrogenase | 60444 |
| MDH5 NADP-dependent | Malate dehydrogenase | 192083 |
| MME1 NAD-dependent | Malic enzyme | 196833 |
| MME2 NADP-dependent | Malic enzyme | 147722 |
| MME3 NADP-dependent | Malic enzyme | 196832 |
| MME4 NADP-dependent | Malic enzyme | 196831 |
| MME5 NADP-dependent | Malic enzyme | 196351 |
| MME6 NADP-dependent | Malic enzyme | 126820 |
| PEPC1 isoform 1 | Phosphoenolpyruvate carboxylase | 80312 |
| PEPC2 isoform 2 | Phosphoenolpyruvate carboxylase | 182821 |
| PYC1 | Pyruvate carboxylase | 112730 |
| PYK1 | Pyruvate kinase | 136854 |
| PYK2 | Pyruvate kinase | 196263 |
| PYK3a, b, c one gene | Pyruvate kinase variants a, b, c | 196261, 107530, 122254 |
| PYK4a, b, c one gene | Pyruvate kinase variants a, b, c | 149896, 119280, 04490 |
| PYK5 | Pyruvate kinase | 118203 |
| PYK6-5/ 6-3 incomplete model but same gene | Pyruvate kinase | 196892, 181547 |

ferredoxin oxidoreductase activity. In *C. reinhardtii*, there are several potential pathways that could lead to the production of succinate. These include the following: (a) pyruvate carboxylation by pyruvate carboxylase to yield oxaloacetate; (b) pyruvate carboxylation by malic enzyme (MME) to yield malate; and (c) phosphoenolpyruvate (PEP) carboxylation by either phosphoenolpyruvate carboxylase (PEPC) or PEP carboxykinase (PCK) to yield oxaloacetate, which can then be reduced to malate by malate dehydrogenase (MDH). The conversion of malate to succinate requires fumarase (FUM) and fumarate reductase (FMR) activities (Fig. 1).

Gene Expression in the Succinate Pathway—Pyruvate is the central fermentation metabolite in *Chlamydomonas*, and altered metabolism of pyruvate could lead to succinate synthesis. To explore the possibility that genes associated with pyruvate metabolism are differentially regulated in the *hydEF-1* mutant, we used qPCR to monitor the abundance of transcripts encoding enzymes potentially involved in metabolizing pyruvate during anaerobic acclimation of the mutant and parental strain (Fig. 1). As shown in Fig. 2, transcripts encoding PFL1 and PFR1 increase significantly in both the mutant and parental strains following the imposition of anaerobic conditions. However, the PFR1 transcript increases more in the parental strain than in the mutant, whereas the PFL1 transcript increases more in the mutant than in the parental strain. This suggests a potential readjustment of the flux of metabolites through the PFL1 and PFR1 pathways during fermentation metabolism. A slight increase in the ratio of formate produced relative to the other secreted metabolites is observed in the mutant strain; however, the total amount of formate secreted is diminished in the mutant relative to the parental strain (Table 1). This finding may reflect decreased fermentative rates in the mutant or competition from the succinate pathway, which becomes active in the mutant (see below).

Although the transcripts level of encoding PFR1 are reduced in the mutant, flux through this pathway may still be required to generate CO₂ for the carboxylation reactions leading to succi-

nate production. This would require ferredoxin to be reoxidized by cellular pathways other than the [FeFe] hydrogenases (e.g. formation of NAD(P)H and/or reduction of sulfite). The fermentative metabolite data indicate that succinate production in the mutant attained a level that is 60–70% of the level that would be produced if all of the CO₂ generated during anaerobic acclimation of the parental strain were used for the synthesis of succinate. These data are suggestive of reduced metabolic flux through the pyruvate ferredoxin oxidoreductase pathway in the mutant; however, pyruvate ferredoxin oxidoreductase activity (at attenuated levels) may still serve to generate the reducing equivalents and CO₂ used to convert the three-carbon metabolites pyruvate and/or phosphoenolpyruvate to four-carbon fermentation products.

Transcripts encoding PEPC1, PYC1, and MME4 increase significantly only in the *hydEF-1* mutant during anaerobiosis (Fig. 2 and supplemental Fig. 1), which suggests that PEPC1 and/or pyruvate carboxylation via PYC1 and/or MME4 may stimulate succinate formation in this strain. Although PFL1, PFR1, PCK1, and PYC1 are encoded by single genes and PEPC by two genes, there are six genes encoding putative malic enzymes. However, only the level of the MME4 transcript increases dramatically (some of the other transcripts increase to a much lesser extent) during anaerobiosis in the mutant strain, with only a small increase in the transcript level in the parental strain (note the differences in the scale for the qPCR results in Fig. 2). These results suggest that MME4 may be predominantly responsible for MME-dependent pyruvate carboxylation during anaerobiosis in the mutant strain. The levels of transcripts encoding PEPC2 and PCK1, enzymes that could also be involved in succinate formation, are not significantly different in the mutant and parental strains (data not shown). Overall, these results suggest that in the absence of active [FeFe] hydrogenases, fermentation metabolites are rerouted away from pyruvate catabolism toward the carboxylation of pyruvate (and perhaps PEP) through PYC1 and MME4 (and perhaps

Flexibility in Anaerobic Metabolism

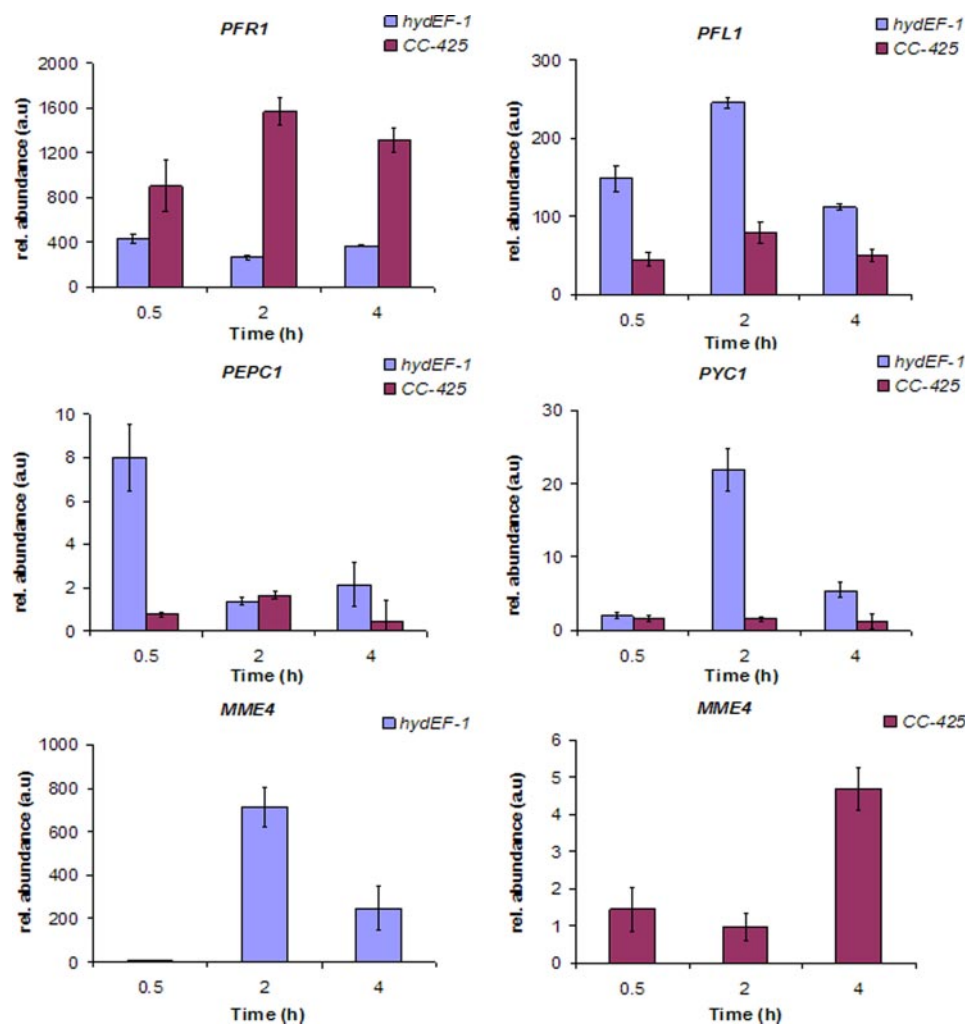


FIGURE 2. Relative level of selected transcripts associated with pyruvate metabolism determined by qPCR at the indicated time of dark, anaerobic acclimation in *hydEF-1* and the parental strain CC-425. Changes in indicated transcript levels following exposure of cells to dark, anaerobic conditions (0.5, 2, and 4 h) are presented as an *n*-fold change (arbitrary units, *a.u.*) relative (*rel.*) to RNA levels at time 0 (just prior to transfer and vigorously oxygenated). The results are normalized to *RACK1* transcript levels, which remained constant over the course of the experiment. The results show the mean \pm S.D. (error bars) for data from three biological (two technical repetitions for each biological replicate) qPCR replicates.

PEPC1). Succinate formation is proposed to proceed via the pathways shown in Fig. 1. This is in accord with the findings that transcripts encoding one of the two *C. reinhardtii* fumarses (FUM1) and the fumarate reductase increase specifically in the mutant but not in the parental strain during anoxia (Fig. 3). Transcripts encoding the MDH enzymes increase to a small extent (particularly MDH2) in response to anaerobiosis, but these increases are similar in the mutant and parental strains (Fig. 3). Together, the qPCR data indicate that the three pathways shown in Fig. 1 for succinate production increase in the *hydEF-1* mutant relative to the parental strain during anaerobiosis.

Attempts to demonstrate *in vitro* succinate formation using cellular extracts of parental and mutant cells were inconclusive. Succinate production was higher in *hydEF-1* extracts relative to the parental strain (data not shown) when supplemented with pyruvate, bicarbonate, and NADH. However, the results were not statistically unequivocal, and we are refining the assay to

optimize both cell breakage and the specific reaction conditions.

Microarray Analyses—Microarray analyses (28, 29) were performed to examine genome-wide differences between the parental strain and the *hydEF-1* mutant during dark, anaerobic acclimation. The previous array data (6) for acclimation of the parental CC-425 strain to dark, anoxic conditions were compared with the current array results obtained for the *hydEF-1* mutant. The relative levels of \sim 10,000 different transcripts (28) were analyzed at various times following exposure of cells to dark, anaerobic conditions. Transcript levels were filtered to capture those for which there was an elevation greater than 1 or a diminution of less than 0.5-fold in relative abundance at 0.5, 2, or 4 h following the imposition of anaerobic conditions. Genes encoding putative fermentative/metabolism proteins with transcripts that accumulated to over 3.0-fold following transfer of mutant cells to anoxic conditions (relative to aerobic control values) are presented in Table 3.

The microarray data (Table 3 and supplemental Table 2) indicate that the majority of metabolic pathways activated during dark, anoxic acclimation in the parental strain (6) are also activated in the mutant. These include transcripts encoding the [FeFe] hydrogenase maturase (HYDG), sulfite reductase, hybrid cluster protein, amylase, and NADH transhydrogenase. Several transcripts encoding enzymes involved in amino acid synthesis and catabolism are also observed to increase, which is consistent with the turnover of proteins involved in aerobic metabolism and the synthesis of proteins required for fermentation metabolism. Increased accumulation of transcripts associated with lipid metabolism was also observed, suggesting that lipid catabolism or reorganization occurs during acclimation to anoxia. Additionally, transcripts encoding fermentative enzymes, such as ACK1 (acetate kinase), PAT2 (phosphate acetyltransferase), pyruvate dehydrogenase kinase, pyruvate decarboxylase, HYDA1, and HYDA2 are observed to increase in both the parental control (6) and the mutant, but only at levels lower than 3-fold in the mutant, and therefore these genes do not appear in Table 3. There are also several transcripts encoding proteins of both known and unknown functions that were observed to increase in the mutant during anoxic acclimation but were not detected in previous microar-

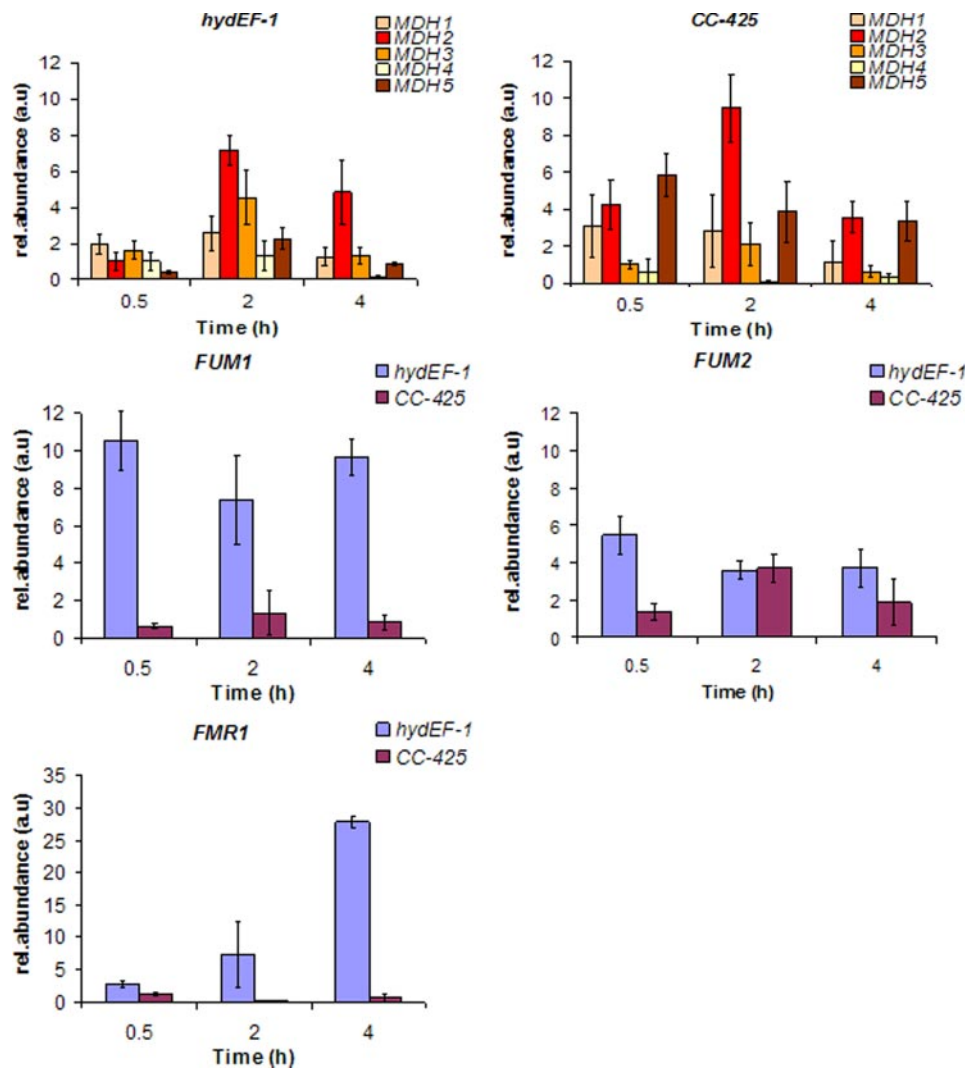


FIGURE 3. Relative level of selected transcripts associated with succinate accumulation determined by qPCR at the indicated time of dark, anaerobic acclimation in *hydEF-1* and the parental strain *CC-425*. Changes in transcript levels following exposure of the cells to dark, anaerobic conditions (0.5, 2, and 4 h) are presented as an *n*-fold change (arbitrary units, a.u.) relative (*rel.*) to RNA levels at time 0 (just prior to transfer and vigorously oxygenated). The results are normalized to *RACK1* transcript levels, which remained constant over the course of the experiment. The results show the mean \pm S.D. (error bars) for data from three biological (two technical repetitions for each biological replicate) qPCR replicates.

ray analyses of anoxia in the parental strain (6). Included among these are several transcripts encoding components of complex I, sulfate adenylyltransferase, Rieske FeS protein, and cytochrome P450.

A second analysis of the microarray data compared transcript abundance in the *hydEF-1* mutant and the parental strain after 4 h of exposure to anaerobic conditions. Table 4 shows the 15 most up-regulated and 10 most significantly down-regulated transcripts encoding putative proteins associated with defined metabolic processes. Among the most significantly up-regulated genes are those encoding nitrate reductase and the hydrogenase maturase HYDG (20). The increase in HYDG is likely a cellular response that reflects the inability of the cell to make an active hydrogenase enzyme. Alternatively, it may be a consequence of the insertional mutation in the adjacent gene, *HYDEF* (20). Nitrate reduction represents an alternative terminal electron acceptor to proton reduction and may be increased in the mutant during anoxia as a mechanism to oxidize reduced ferre-

doxin that is generated by PFR1. Likewise, sulfate activation and reduction would be a way of eliminating intracellular reducing equivalents. As shown in Table 4, transcripts encoding sulfate adenylyltransferase, which catalyzes the first step of both the assimilatory and dissimilatory sulfate reduction pathways, accumulates to significantly higher levels in the mutant relative to the parental control. The conversion of sulfite to sulfide is catalyzed by sulfite reductase, whose transcripts increase during anoxia in both the mutant and parental strains. Additional fermentation transcripts encoding proteins associated with NADH oxidation/reduction and ATP synthesis/transport are differentially regulated, which is consistent with hydrogenase activity influencing the relative levels of NADH and ATP during anoxia. Interestingly, components of both mitochondrial complex I and cytochrome *b₆f* are differentially up-regulated in the mutant, suggesting that the redox status of these electron transport chains has been altered in the *hydEF-1* mutant. Several genes, encoding some MMEs, FMR1, and PCK1, were not represented on the array.

DISCUSSION

The flexibility of algal metabolism is of interest for developing an informed understanding of the following: (a) metabolite exchange in natural microbial communities; (b) the role of unicellular algae in global carbon cycling; and (c) strategies for engineering phototrophic microorganisms for renewable energy production (11, 30–33). The *C. reinhardtii* genome sequence has provided gene models for populating previously documented metabolic pathways, revealed a diversity of predicted metabolisms, provided insights into the evolution of the green algal lineage, and indicated that parallel processes may occur in multiple cellular compartments (5, 6). An intriguing aspect of algal physiology is the ways in which these organisms acclimate to anoxia (8, 9, 34, 35), which likely occurs as a consequence of microbial respiration at night in environments that are not well oxygenated (e.g. soil environment from which *C. reinhardtii* was originally isolated). Several research efforts are currently focused on developing a more comprehensive understanding of anoxic metabolism in this alga to support future efforts to generate H₂, organic acids, and/or ethanol. Hydrogenase activity in *C. reinhardtii* has been the focus of extensive research because it cat-

Flexibility in Anaerobic Metabolism

TABLE 3

Transcripts associated with metabolism/fermentation showing at least a ≥ 3.0 -fold change in abundance in at least one time point following the transfer of *hydEF-1* mutant cells from light, aerobic conditions to dark, anaerobic conditions

Also shown is the identification number of the oligonucleotide, the protein ID, and the associated annotation from the JGI browser. Shaded transcripts are similarly upregulated in the parental strain.

| Oligo ID ^a | Protein ID ^b | Annotation | Fold change in transcript abundance ^{c,d,e} | | | | | |
|--------------------------------|-------------------------|---|--|----------|-----|----------|-----|----------|
| | | | 0.5h | t-test | 2h | t-test | 4h | t-test |
| <i>Metabolism/Fermentation</i> | | | | | | | | |
| 132.A | 196226 | HYDG, hydrogenase assembly factor | 3.2 | 1.22E-01 | 9.5 | 1.08E-01 | 5.0 | 7.50E-02 |
| 202.A | 83064 | PGH1, enolase | 2.8 | 3.23E-02 | 2.8 | 2.31E-02 | 3.1 | 3.83E-02 |
| 9407.E | 147722 | MME2, NADP dependent malic enzyme | 2.1 | 1.02E-01 | 3.2 | 1.39E-01 | 3.0 | 2.26E-01 |
| 9624.C | 181846 | Keto-acid reductoisomerase | 5.5 | 0.28E-01 | 2.0 | 5.00E-02 | 11 | 0.43E-01 |
| 1998.C | 157654 | DUR2, urea carboxylase | 1.6 | 1.36E-01 | 3.1 | 2.09E-01 | 2.1 | 2.26E-01 |
| 1185.C | 159263 | End of acetyl-CoA carboxylase/ biotin decarboxylase | 2.1 | 1.03E-01 | 3.4 | 1.41E-01 | 2.7 | 2.87E-01 |
| 9432.E | 165130 | Lysine decarboxylase-like protein | 3.4 | 1.32E-01 | 10 | 8.80E-02 | 5.5 | 3.14E-01 |
| 2622.C | 146556 | Multicopper oxidase, type 1 | 2.8 | 2.31E-01 | 5.5 | 1.91E-01 | 9.0 | 3.61E-01 |
| 9674.E | 192232 | Sulfite reductase | 3.9 | 1.96E-01 | 4.2 | 7.86E-01 | 3.8 | 2.17E-01 |
| 144.A | 184661 | NIT1, nitrate reductase | 4.2 | 2.40E-01 | 6.2 | 2.32E-01 | 4.5 | 2.68E-01 |
| 468.A | 154650 | AT51, sulfate adenyl transferase | 2.9 | 7.01E-02 | 2.3 | 1.12E-01 | 4.7 | 2.72E-01 |
| 1054.C | 191051 | PAT2, phosphate acetyl transferase | 3.6 | 2.03E-02 | 2.2 | 1.87E-02 | 2.0 | 3.21E-02 |
| 9383.C | 148255 | HCP4, hybrid cluster protein | 1.4 | 2.20E-02 | 2.0 | 3.50E-02 | 3.3 | 3.24E-02 |
| 9552.E | 157360 | Esterase/lipase | 2.5 | 1.68E-01 | 2.7 | 2.73E-01 | 4.0 | 3.13E-01 |
| 1265.C | 129982 | ACK1, acetate kinase | 2.2 | 1.37E-01 | 4.2 | 1.52E-01 | 4.9 | 1.03E-01 |
| 9744.E | 154478 | Glutamate 5-kinase | 4.4 | 8.97E-02 | 5.7 | 1.25E-01 | 5.2 | 2.43E-01 |
| 616.C | 169030 | Tyrosine-protein kinase | 4.6 | 1.46E-01 | 4.0 | 2.41E-01 | 7.1 | 2.64E-01 |
| 192.A | 196943 | VPS34, Phosphatidylinositol 3-kinase | 2.5 | 3.19E-01 | 3.2 | 1.09E-01 | 3.6 | 3.52E-01 |
| 1209.C | 196261 | PYK3, Pyruvate kinase | 3.0 | 1.37E-01 | 4.7 | 1.03E-01 | 3.0 | 4.88E-01 |
| 4361.C | 196383 | PGK2, phosphoglycerate kinase | 4.1 | 1.81E-01 | 4.2 | 2.11E-01 | 4.4 | 1.40E-01 |
| 31.A | 129128 | RIP1, rieske iron-sulfur protein, ubiquinol-cytochrome c reductase | 2.5 | 1.06E-01 | 4.6 | 1.34E-01 | 2.2 | 2.28E-01 |
| 9278.E | 196742 | CYP97A5, cytochrome P450 | 2.2 | 2.61E-01 | 3.6 | 2.92E-01 | 2.4 | 4.07E-01 |
| 9503.E | 139758 | NAD(P) transhydrogenase | 1.6 | 2.70E-01 | 1.8 | 1.20E-02 | 6.7 | 3.06E-01 |
| 9844.E | 142838 | Aminoacidipate-semialdehyde dehydrogenase-phosphopantetheinyl transferase | 3.1 | 2.36E-01 | 4.3 | 4.14E-02 | 2.4 | 4.37E-01 |
| 216.A | 59411 | NUO8, NADH:ubiquinone oxidoreductase subunit | 6.0 | 4.14E-01 | 2.4 | 1.84E-01 | 1.8 | 4.43E-01 |
| 108.A | 131464 | NUO17, NADH: ubiquinone oxidoreductase subunit | 5.0 | 1.83E-01 | 13 | 2.06E-01 | 6.7 | 1.84E-01 |
| 140.A | 186342 | NUO6, NADH:ubiquinone oxidoreductase subunit | 4.7 | 8.20E-02 | 3.0 | 1.42E-02 | 4.3 | 2.88E-01 |
| 487.A | 127639 | NUOB13, NADH:ubiquinone oxidoreductase | 1.5 | 4.50E-01 | 1.5 | 4.69E-01 | 3.9 | 5.37E-01 |
| 8375.D | 195735 | NDA7, putative type-II NADH dehydrogenase | 3.9 | 3.69E-01 | 3.7 | 2.80E-01 | 3.7 | 3.69E-01 |
| 9411.E | 194856 | 5, 10-methylenetetrahydrofolate dehydrogenase | 3.9 | 1.96E-01 | 4.2 | 7.86E-01 | 3.8 | 2.81E-01 |
| 7842.D | 146556 | Proline dehydrogenase | 4.8 | 1.22E-01 | 2.7 | 1.65E-01 | 4.0 | 2.07E-01 |
| 7341.C | 130769 | Homoserine dehydrogenase | 2.5 | 3.06E-01 | 5.5 | 2.75E-01 | 8.6 | 2.18E-01 |
| 7632.D | 78757 | PGD1, D-3-phosphoglycerate dehydrogenase | 2.2 | 9.76E-02 | 6.5 | 1.71E-01 | 5.5 | 2.90E-01 |
| 5158.C | 166040 | GPD1, glycerol-3-phosphate dehydrogenase | 2.4 | 2.13E-01 | 3.6 | 9.26E-02 | 2.0 | 1.65E-01 |
| 9202.E | 135609 | Aldehyde dehydrogenase | 2.9 | 1.50E-01 | 1.6 | 4.12E-01 | 3.4 | 4.79E-01 |
| 9898.E | 153682 | GDH2, glutamate dehydrogenase | 2.0 | 2.52E-01 | 4.5 | 8.77E-02 | 4.5 | 1.99E-01 |
| 8562.D | 152239 | PYR4, dihydroorotate dehydrogenase | 2.0 | 1.45E-01 | 3.2 | 1.40E-01 | 2.1 | 1.62E-01 |
| 4416.C | 79471 | OGD1, 2-oxoglutarate dehydrogenase | 2.6 | 1.41E-01 | 3.5 | 3.39E-01 | 2.7 | 3.69E-01 |
| 1259.C | 128289 | Acyl-CoA dehydrogenase | 1.8 | 2.68E-01 | 3.0 | 2.75E-02 | 2.1 | 1.20E-02 |
| 1275.C | 118204 | Acetoacetyl-CoA-S-thiolase | 2.3 | 1.33E-01 | 4.5 | 9.31E-02 | 4.4 | 2.84E-01 |
| 2186.C | 196483 | METC, cystathionine β -lyase | 4.4 | 1.47E-01 | 3.6 | 9.63E-02 | 1.8 | 3.95E-01 |
| 1454.C | 128032 | SUFS2, cysteine desulfurase | 1.2 | 2.18E-01 | 3.6 | 1.90E-01 | 2.4 | 1.53E-01 |
| 639.C | 186880 | HIS3, imidazolglycerol-phosphate dehydratase | 2.2 | 1.49E-01 | 2.4 | 1.23E-01 | 9.8 | 1.49E-01 |
| 226.A | 168551 | MAS, malate synthase glyoxysomal | 1.8 | 2.81E-01 | 3.7 | 1.04E-01 | 2.7 | 2.64E-01 |
| 5619.C | 205746 | GSN1, NADH-dependent glutamate synthase | 3.2 | 3.86E-01 | 2.7 | 1.92E-01 | 1.3 | 4.65E-01 |
| 9194.E | 140252 | Asparagine synthase | 3.2 | 7.72E-02 | 4.7 | 1.08E-01 | 2.3 | 2.37E-01 |
| 816.C | 127384 | Threonine synthase | 2.3 | 1.04E-01 | 3.3 | 7.01E-02 | 5.5 | 0.43E-01 |
| 1428.C | 139742 | Bifunctional dihydrofolate reductase-thymidylate synthase | 1.8 | 3.40E-01 | 3.6 | 8.05E-02 | 2.4 | 3.05E-01 |
| 9347.E | 5137 | ALSS1, acetolactate synthase | 1.8 | 2.23E-01 | 3.7 | 1.33E-01 | 2.7 | 1.38E-01 |
| 9887.E | 162404 | Dihydrodipicolinate synthase | 1.2 | 3.94E-01 | 3.6 | 1.01E-01 | 2.5 | 2.29E-01 |
| 3322.C | 178232 | AMD1, α -1,2-mannosidase | 0.9 | 2.03E-01 | 1.0 | 4.19E-01 | 3.0 | 2.49E-01 |
| 9965.E | 56237 | FAD7, Ω -3 fatty acid desaturase | 2.3 | 1.83E-01 | 3.3 | 2.50E-01 | 2.4 | 1.39E-01 |
| 8149.D | 182572 | Δ 5 fatty acid desaturase | 3.6 | 2.07E-01 | 1.9 | 1.62E-01 | 1.7 | 2.73E-01 |
| 20.A | 82495 | Fructose-biphosphate aldolase 1 | 3.4 | 1.08E-01 | 2.0 | 2.89E-01 | 5.5 | 3.21E-01 |
| 49.A | 164593 | STA6, ADP-glucose pyrophosphorylase | 1.4 | 2.61E-01 | 1.4 | 3.96E-01 | 3.6 | 3.35E-01 |
| 215.A | 503 | STA2, granule-bound starch synthase | 4.5 | 2.34E-01 | 1.7 | 2.74E-01 | 1.6 | 5.63E-01 |
| 8376.D | 132067 | ISA3, isoamylase-like protein | 1.5 | 9.77E-02 | 3.0 | 2.09E-01 | 1.7 | 2.67E-01 |
| 7498.C | 129211 | AMYB3, β -amylase | 3.0 | 1.73E-01 | 5.1 | 3.86E-01 | 7.6 | 2.82E-01 |
| 3762.C | 112511 | AMYB2, β -amylase | 2.5 | 2.73E-01 | 2.6 | 2.18E-01 | 6.2 | 3.69E-01 |
| 8602.D | 129524 | UDP-glucose 6-dehydrogenase | 2.1 | 1.97E-01 | 3.3 | 4.90E-01 | 1.2 | 4.97E-01 |

^a Identification number of the oligonucleotide sequence used to make the array element is shown.

^b Identification number of protein generated from the corresponding gene model (JGI *C. reinhardtii* version 3.0 is shown).

^c Change in transcript abundance at 0.5, 2, and 4 h after transferring cells to dark, anaerobic conditions relative to time 0 (just prior to transfer) is shown.

^d Average of three experimental replicates for time point 0.5 h, and four experimental replicates for time points 2 and 4 h. Two technical repetitions were done for each experimental repetition (each slide contained each array element in duplicate).

^e Student's *t* test is shown.

TABLE 4

The 15 most highly up-regulated and 10 most significantly down-regulated transcripts associated with metabolism in the *hydEF-1* mutant relative to the CC-425 parental strain after 4 h of dark, anaerobic acclimation

Both the protein ID and associated annotation from the JGI browser are given. Shaded transcripts are significantly upregulated in the parental strain.

| Oligo ID ^a | Protein ID ^b | Annotation | Fold change in transcript abundance <i>hydEF-1</i> /WT ^{c,d} | |
|--|-------------------------|---|---|----------|
| | | | 4h | t-test |
| <i>Fermentation/Metabolism/electron transfer</i> | | | | |
| up regulated genes | | | | |
| 216.A | 59411 | NUOA8, NADH:ubiquinone oxidoreductase subunit | 34 | 9.25E-03 |
| 163.A | 76602 | ATP1, mitochondrial F1F0 ATP synthase α subunit | 21 | 1.09E-04 |
| 9168.E | 158121 | Putative mitochondria malonyl-CoA decarboxylase | 18 | 1.62E-02 |
| 9202.E | 135609 | Aldehyde dehydrogenase | 16 | 3.90E-04 |
| 468.A | 183942 | ATS1, sulfate adenylyltransferase | 15 | 4.38E-04 |
| 9411.E | 743 | Tetrahydrofolate, dehydrogenase cyclohydrolase | 14 | 1.34E-01 |
| 404.A | 185971 | PET0, cytochrome B6-F complex subunit O | 13 | 2.99E-02 |
| 202.A | 83064 | PGH, 1 enolase | 13 | 4.93E-03 |
| 5154.C | 188027 | ADP/ATP carrier protein | 11 | 3.34E-03 |
| 226.A | 168551 | MAS, malate synthase | 10 | 4.39E-03 |
| 3762.C* | 112511 | AMYB2, β -amylase | 14 | 1.64E-02 |
| 358.A | 184661 | NIT1, nitrate reductase | 10 | 9.90E-04 |
| 2622.C | 146556 | Multicopper oxidase type 1 | 9.2 | 4.46E-02 |
| 132.A | 196226 | HYDG, [FeFe]-hydrogenase maturase | 7.4 | 7.21E-02 |
| 6449.C | 186369 | PIS1, phosphatidylinositol synthase | 6.8 | 7.19E-02 |
| down regulated genes | | | | |
| 428.A* | 192090 | Putative nitrate transporter component | 0.1 | 9.48E-02 |
| 3999.C | 180226 | Putative spermidine synthase | 0.1 | 2.82E-01 |
| 73.A | 170364 | Putative ARS2-like | 0.1 | 3.79E-01 |
| 3159.C | 191051 | PAT2, phosphotransacetylase | 0.1 | 9.05E-02 |
| 6695.C | 192731 | Putative arylsulfatase 2 precursor | 0.1 | 3.98E-01 |
| 1591.C | 153269 | Putative PsaB | 0.1 | 2.36E-01 |
| 7276.C | 190510 | Electron transport protein/ putative mannitol dehydrogenase | 0.1 | 3.37E-01 |
| 551.C | 154128 | Electron transport protein/ Putative cytochrome P450 | 0.2 | 2.47E-01 |
| 6203.C | 150732 | RMT2, putative ribulose 1,5 bisphosphate carboxylase/oxygenase N-methyl transferase subunit | 0.2 | 4.16E-01 |
| 7003.C | 157451 | ATPA, chloroplastic ATP synthase α subunit | 0.3 | 7.39E-02 |

^a Identification number of the oligonucleotide sequence used to make the array element is shown.

^b Identification number of protein generated from the corresponding gene model (JGI *C. reinhardtii* version 3.0 is shown).

^c Change in transcript abundance at 4 h after transferring cells to dark, anaerobic conditions relative to time 0 h (just prior to transfer) is shown.

^d Average of three experimental repetitions (two technical repetitions for each experimental repetition) is shown.

^e Student's *t* test is shown.

* Genes differentially regulated in the *hydEF-1* mutant versus CC-425 in standard culture conditions (TAP, light, aerobic conditions); 428.A (0 h, 5.21; *t* test, 2.79E-02); 3762.C (0 h, 7.45; *t* test, 5.52E-02) are shown.

analyzes the production of the renewable energy carrier H₂ (4, 33, 36–41). To further study the role of hydrogenases in algal physiology and to define the metabolic adjustments induced by the loss of hydrogenase activity, physiological responses observed during anoxic acclimation of a *C. reinhardtii* mutant lacking hydrogenase activity were examined relative to the parental strain. Interestingly, rather than causing an increased metabolic flux into alternative pathways operating at significant levels in the parental strain, activation of new metabolic pathways leading to succinate accumulation were observed. The ability of *C. reinhardtii* to switch to a pathway that is minimally active in the parental strain, continues to demonstrate the metabolic versatility of this alga and its ability to alter its metabolism in response to environmental change.

Succinate Accumulation—The increased production of succinate, the absence of H₂ production, and the decreased evolu-

tion of CO₂ were the most significant metabolic differences observed in the *hydEF-1* mutant relative to the parental strain during dark, anoxic acclimation. In the mutant, decreased CO₂ evolution and increased abundance of transcripts encoding proteins able to carboxylate pyruvate, congruent with succinate production, suggest that in the absence of hydrogenase activity, pyruvate is carboxylated to generate either malate and/or oxaloacetate. These metabolites are putatively converted into succinate as depicted in Fig. 1. Both malic enzyme and pyruvate carboxylase use CO₂ as a substrate to carboxylate pyruvate, and the activity of either or both may be responsible for the nearly steady state levels of CO₂ observed in the mutant. Transcripts encoding both of these enzymes increase significantly in the mutant strain during anoxic acclimation. Although the malic enzyme typically decarboxylates malate generating pyruvate, examples of malic enzymes functioning in the reverse direction

Flexibility in Anaerobic Metabolism

have been reported (42–44). Overexpression of the gene (*scfA*) encoding the malic enzyme in *Escherichia coli* leads to succinate accumulation in a mutant background with elevated pyruvate levels resulting from disruptions of the genes encoding both lactate dehydrogenase and PFL (43, 44). Of the *C. reinhardtii* malic enzymes, SfcA is most similar to MME4.

Pyruvate carboxylation can also proceed via pyruvate carboxylase to form oxaloacetate, and transcripts encoding PYC1 increase during anoxia in the mutant. However, the transcripts of five putative MDH enzymes, required for the conversion of oxaloacetate into malate and subsequently succinate, do not increase dramatically in the mutant relative to the parental strain. Furthermore, the level of the PYC1 transcript increases ~20-fold, whereas the *MME4* transcript increases in abundance by over 500-fold in the mutant. Based on the qPCR C_t values for the six *MME* genes, *MME4* transcripts are least abundant under oxic conditions in both the parental strain and the *hydEF-1* mutant. The relatively strong induction of *MME4* compared with *PYC1* and *MDH* transcripts suggests that *MME4* may be responsible for the majority of increased metabolic flux toward succinate production. An alternative pathway to succinate via PEPC1 may be modestly activated, based on transcript levels. In addition to PEPC, the conversion of phosphoenolpyruvate to oxaloacetate could also potentially proceed via PCK (43); however, this pathway does not appear to contribute to fermentative succinate formation in *E. coli* (45), and we do not observe significant differential regulation of the PCK1 transcript in *C. reinhardtii* (data not shown). Transcripts encoding fumarase and fumarate reductase, required for the conversion of malate to succinate, increase significantly only in the mutant during anoxic acclimation, which is consistent with activation of the pathway shown in Fig. 1; *MME4* would carboxylate pyruvate to generate malate, which could then be metabolized to succinate by the activities of FUM and FMR. Elevated succinate production in the mutant provides a means to reoxidize cellular reductant to sustain additional rounds of anaerobic glucose catabolism. Moreover, ATP production is maintained by the conversion of PEP to pyruvate and subsequent carboxylation by malic enzyme. The pathways shown in Fig. 1 reflect whole-cell metabolic networks. To better understand the fermentative metabolism of *C. reinhardtii*, it will be important to experimentally establish the compartmentalization of the individual enzymes. We have used existing proteomic data (5, 46) and *in silico* analysis of peptide localization sequences to derive putative localizations, as shown in Fig. 1. However, it should be cautioned that the *in silico* predictions are highly speculative.

Anoxic Metabolism—Although transcripts encoding PFR1 are observed to increase in the mutant during anoxic acclimation, their levels are significantly reduced relative to the parental strain. This may be a consequence of the inability of hydrogenase to oxidize ferredoxin and restricted metabolic flux through the PFR1 pathway. Intriguingly, in parental cells, the amount of H_2 detected is significantly less (~10 times less) than the amount of CO_2 released under our experimental conditions. If PFR1 were solely responsible for the production of CO_2 , and if ferredoxin were reoxidized exclusively by hydrogenase to produce H_2 , then dark, fermentative levels of H_2 and

CO_2 should be equal. The significantly reduced H_2 levels relative to CO_2 indicate that other enzymes such as ferredoxin-NAD(P)H oxidoreductases or perhaps sulfite or nitrite reductases may also be responsible for oxidizing ferredoxin. Additional enzymes such as pyruvate decarboxylase may also contribute to CO_2 levels. Redox calculations based on the assumption that all secreted metabolites quantified in Table 1 are derived from starch/glucose indicate that ~1.6 mM of electron reducing equivalents are not reoxidized by the observed metabolites in the parental strain. These could be reoxidized if 0.2 mM sulfate, which is present in TAP medium, were reduced to sulfide. Moreover, anabolic pathways such as lipid synthesis could also play a role in oxidizing these reducing equivalents. In the case of the *hydEF-1* mutant, there is an excess of metabolites relative to the amount of NADH available; however, this can be accounted for if reducing equivalents (and CO_2) from PFR1 activity are used in the synthesis of succinate.

It is also perplexing that in parental cells, the ratio of acetate to ethanol is not equal (Table 1). If these fermentation metabolites were all derived from acetyl-CoA, these ratios should be approximately equal, or other mechanisms to oxidize NADH must be triggered that establish a $NAD^+/NADH$ stoichiometry that sustains glycolysis (Fig. 1). Because the cells were cultured in TAP medium, which contains acetate (some of which remained in the medium at the time of cell harvesting), it is likely that some of the measured acetate originated from the medium rather than from pyruvate metabolism. Secretion of medium-derived acetate by cells at the onset of anaerobiosis is consistent with high levels of this organic acid at the 0.5-h time point (Table 1) relative to other fermentative metabolites. If the majority of acetate in the medium at 0.5 h is not derived from starch degradation, then the fermentation stoichiometry more closely approximates the formate/acetate/ethanol stoichiometry of 2:1:1 reported by others (7, 13). However, even if we adjust our calculations and assume that most of the acetate at 0.5 h is medium-derived, the sum of acetate and ethanol still remains slightly in excess of the detected levels of formate. This finding is consistent with CO_2 production coming from pyruvate decarboxylation which, if mediated by PFR1, could contribute to the production of fermentative H_2 in the parental strain.

The pathways leading to succinate production require CO_2 input, which likely originates from the following: (a) PFR1; (b) PDC; (c) pyruvate dehydrogenase during anoxic acclimation when cells are metabolizing residual O_2 ; or (d) reserves of bicarbonate that accumulate within cells during aerobic culturing. It is likely that PFR1 is still active to an extent and that CO_2 produced by this pathway is used to carboxylate pyruvate or PEP. Ferredoxin could then potentially be used to generate NAD(P)H for succinate production. Together, the data suggest that although hydrogenase activity does not appear to be exclusively responsible for ferredoxin oxidation in the parental strain, its absence in cells that have acclimated to dark, anoxic conditions causes the activation of metabolic pathways leading to succinate synthesis. As the amount of succinate produced in the mutant exceeds the H_2 produced by the parental strain by 5–10-fold, the rerouting of metabolites does not simply compensate at a stoichiometric level for the loss of the electron valve activity of the hydrogenase. Regulatory processes must become

active that generate a new cellular homeostasis. The regulators that control this process have not been identified, although it is conceivable that the loss of hydrogenase activity results in increased cellular reductant that signals changes in gene expression via reduced NAD(P) or redox sensors such as thioredoxins (47, 48).

Transcriptome—The microarray data are consistent with the development of fermentation metabolism during dark anaerobiosis in both the mutant and parental strains. Transcripts encoding the hydrogenase maturation factor HYDG, and starch and pyruvate-catabolizing enzymes, including amylases, acetate kinase, pyruvate kinase, and phosphate acetyltransferase, all increase in the mutant and parental strains. Moreover, transcripts for pyruvate dehydrogenase kinase, which phosphorylates and inhibits pyruvate dehydrogenase, also increases in the mutant relative to the parental strain. The pyruvate dehydrogenase complex oxidizes pyruvate-forming NADH, acetyl-CoA, and CO₂ during aerobic metabolism, and inhibition of pyruvate dehydrogenase redirects pyruvate metabolism into fermentation pathways.

Dark anaerobiosis also elicits an increase in the abundance of several transcripts encoding enzymes involved in amino acid catabolism or synthesis, such as lysine decarboxylase, proline dehydrogenase, glutamate kinase, threonine synthase, cystathionine β -lyase, and asparagine synthase. This is likely a function of proteome reorganization as enzymes used in aerobic metabolism are degraded, and fermentation enzymes are synthesized. Transcripts also increase for cysteine desulfurase, an enzyme that mobilizes sulfide for the formation of FeS clusters that would be required by several fermentative FeS proteins, including ADH1, PFLA1, and PFR1.

The microarray data also indicate that dark anaerobiosis leads to increases in transcripts encoding subunits of the mitochondrial NADH-oxidizing complex I, including *NUIO8*, which appears to be the most differentially up-regulated gene in the mutant relative to the parental strain after 4 h of anoxic acclimation. Other significant differences between the mutant and the parental strain include increases in levels of transcripts in the mutant for nitrate reductase (NIT1) and the sulfate adenylyltransferase. *ATS1* activates sulfate for subsequent reduction. Sulfite reductase transcripts also increase during anaerobiosis. Reductions of nitrate, sulfate, and fumarate have all been linked to anaerobic respiration, where these substrates replace O₂ as alternative electron acceptors (49–51) and the reductive process can be electrogenically coupled to the production of ATP in some instances (52–54). This method of ATP production, in addition to substrate level phosphorylation, can provide a substantial source of energy for certain organisms during anaerobiosis. Although it is tempting to conclude that increases in transcripts encoding components of complex I, NIT1, *ATS1*, sulfite reductase, and fumarate reductase reflect activation of components of anaerobic respiration induced in response to anoxia, it should be noted that most of these *C. reinhardtii* enzymes are not typically associated with anaerobic respiration. In the case of nitrate and sulfite reductases, each enzyme is most similar to assimilatory enzymes used in biosynthetic pathways. Moreover, in the case of NIT1, the cells were cultured in TAP medium, which does not contain nitrite/nitrate, and the *C.*

reinhardtii genome does not appear to encode the enzyme ammonia monooxygenase, the first step in ammonia oxidation (55). It is therefore difficult to envision, under our experimental conditions, the origin of nitrite/nitrate. However, the conditions used in these studies neither reflect the variety of nutrient and temperature conditions experienced in the environment nor the multitude of direct and indirect interactions among the organisms that populate soil environments. Interestingly, the addition of nitrate to the *C. reinhardtii* culture medium suppresses H₂ production (56), suggesting that the cells have the capacity to use substrates such as nitrate and perhaps sulfate as terminal electron acceptors during anaerobiosis, and thiosulfate formation has been reported in anaerobic extracts of *C. reinhardtii* (57).

It is also possible that differences in the levels of specific transcripts in the mutant relative to the parental strain reflect more general regulatory and signaling mechanisms. These differences may be elicited in response to the overall increase in abundance of intracellular reducing equivalents that result from both a loss of hydrogenase activity and anaerobiosis. This physiological state may mirror cells experiencing specific conditions, which are often dynamic, in the natural environment. Experimental conditions used in the laboratory are less dynamic and often artificial relative to what *C. reinhardtii* would experience in the environment. For these studies, aerobic cultures were illuminated, stirred, and vigorously aerated by bubbling with a mixture of CO₂-enriched air, which favors high photosynthetic activity and aerobic respiration. Furthermore, anaerobic samples were rigorously controlled to exclude all O₂. In natural settings, the transition from aerobic conditions to anaerobiosis is likely more gradual, and increased expression of some genes encoding polypeptides, such as those of complex I, may reflect regulatory responses that have evolved to oxidize cellular reductant during a transition first to hypoxia, rather than to complete anoxia. A much more comprehensive understanding of anoxic cellular processes, accurate subcellular localization of relevant enzymes, and a detailed understanding of metabolite exchange between organelles is required for the following: (a) to develop an improved understanding of hydrogenase activity in cellular metabolism during dark anaerobiosis; (b) to determine whether other potential terminal electron acceptors, such as nitrate and sulfate, function to alleviate intracellular redox stress; and (c) to examine whether enhanced expression of some genes, as revealed by microarray analyses, translates into increased enzymatic activity.

Summary—In summary, the fermentative metabolism of *C. reinhardtii* has been shown to readily accommodate the loss of hydrogenase activity by synthesizing succinate, which would contribute to the reoxidation of NADH and sustain glycolysis for the production of ATP during anaerobiosis. Activation of this pathway, which is minimally active in the parental strain (based on transcript and metabolite analyses), further illustrates the metabolic flexibility of *C. reinhardtii*, an alga that appears to be well adapted to withstand a variety of environmental challenges, including anoxia. It is possible that the ability to synthesize succinate in the absence of hydrogenase activity reflects an adaptation used in natural settings in which fermentation metabolism is elicited under conditions in which

hydrogenase activity is inhibited (e.g. brief exposures to gases such as CO or O₂, which are likely not strictly excluded in certain environments). The transcriptome data indicate that the loss of hydrogenase activity results in the increased expression of several transcripts associated with a variety of cellular redox processes. Some of these processes have been associated with aerobic respiration, indicating that there are still several aspects of anoxic acclimation that are not fully understood and warrant further investigation. The metabolic capacity of *C. reinhardtii*, particularly during anaerobiosis, is extremely versatile and complicated. This alga readily responds to variations in culturing and assay conditions in ways that we are just beginning to elucidate. The availability of the *C. reinhardtii* genome sequence, high throughput omics-based approaches, and mutants disrupted in a variety of cellular process will provide the foundation to further examine and understand the metabolic flexibility of this fascinating phototroph.

REFERENCES

- Merchant, S. S., Prochnik, S. E., Vallon, O., Harris, E. H., Karpowicz, S. J., Witman, G. B., Terry, A., Salamov, A., Fritz-Laylin, L. K., Marechal-Drouard, L., Marshall, W. F., Qu, L. H., Nelson, D. R., Sanderfoot, A. A., Spalding, M. H., Kapitonov, V. V., Ren, Q., Ferris, P., Lindquist, E., Shapiro, H., Lucas, S. M., Grimwood, J., Schmutz, J., Cardol, P., Cerutti, H., Chanfreau, G., Chen, C. L., Cognat, V., Croft, M. T., Dent, R., Dutcher, S., Fernandez, E., Fukuzawa, H., Gonzalez-Ballester, D., Gonzalez-Halphen, D., Hallmann, A., Hanikenne, M., Hippler, M., Inwood, W., Jabbari, K., Kalanon, M., Kuras, R., Lefebvre, P. A., Lemaire, S. D., Lobanov, A. V., Lohr, M., Manuell, A., Meier, I., Mets, L., Mittag, M., Mittelmeier, T., Moroney, J. V., Moseley, J., Napoli, C., Nedelcu, A. M., Niyogi, K., Novoselov, S. V., Paulsen, I. T., Pazour, G., Purton, S., Ral, J. P., Riano-Pachon, D. M., Riekhof, W., Rymarquis, L., Schroda, M., Stern, D., Umen, J., Willows, R., Wilson, N., Zimmer, S. L., Allmer, J., Balk, J., Bisova, K., Chen, C. J., Elias, M., Gendler, K., Hauser, C., Lamb, M. R., Ledford, H., Long, J. C., Minagawa, J., Page, M. D., Pan, J., Pootakham, W., Roje, S., Rose, A., Stahlberg, E., Terauchi, A. M., Yang, P., Ball, S., Bowler, C., Dieckmann, C. L., Gladyshev, V. N., Green, P., Jorgensen, R., Mayfield, S., Mueller-Roeber, B., Rajamani, S., Sayre, R. T., Brokstein, P., Dubchak, I., Goodstein, D., Hornick, L., Huang, Y. W., Jhaveri, J., Luo, Y., Martinez, D., Ngau, W. C., Otilar, B., Poliakov, A., Porter, A., Szajkowski, L., Werner, G., Zhou, K., Grigoriev, I. V., Rokhsar, D. S., and Grossman, A. R. (2007) *Science* **318**, 245–250
- Grossman, A. R., Croft, M., Gladyshev, V. N., Merchant, S. S., Posewitz, M. C., Prochnik, S., and Spalding, M. H. (2007) *Curr. Opin. Plant Biol.* **10**, 190–198
- Kosourov, S., Seibert, M., and Ghirardi, M. L. (2003) *Plant Cell Physiol.* **44**, 146–155
- Ghirardi, M. L., Posewitz, M. C., Maness, P.-C., Dubini, A., Yu, J., and Seibert, M. (2007) *Annu. Rev. Plant Biol.* **58**, 71–91
- Atteia, A., van Lis, R., Gelius-Dietrich, G., Adrait, A., Garin, J., Joyard, J., Rolland, N., and Martin, W. (2006) *J. Biol. Chem.* **281**, 9909–9918
- Mus, F., Dubini, A., Seibert, M., Posewitz, M. C., and Grossman, A. R. (2007) *J. Biol. Chem.* **282**, 25475–25486
- Gfeller, R. P., and Gibbs, M. (1984) *Plant Physiol.* **75**, 212–218
- Steunou, A. S., Bhaya, D., Bateson, M. M., Melendrez, M. C., Ward, D. M., Brecht, E., Peters, J. W., Kuhl, M., and Grossman, A. R. (2006) *Proc. Natl. Acad. Sci. U. S. A.* **103**, 2398–2403
- Melis, A., Zhang, L., Forestier, M., Ghirardi, M. L., and Seibert, M. (2000) *Plant Physiol.* **122**, 127–136
- Kruse, O., Rupprecht, J., Mussgnug, J. H., Dismukes, G. C., and Hankamer, B. (2005) *Photochem. Photobiol. Sci.* **4**, 957–970
- Hankamer, B., Lehr, F., Rupprecht, J., Mussgnug, J. H., Posten, C., and Kruse, O. (2007) *Physiol. Plant* **131**, 10–21
- Hemschemeier, A., and Happe, T. (2005) *Biochem. Soc. Trans.* **33**, 39–41
- Kreutzberg, K. (1984) *Physiol. Plant.* **61**, 87–94
- Ohta, S., Miyamoto, K., and Miura, Y. (1987) *Plant Physiol.* **83**, 1022–1026
- Hemschemeier, A., Jacobs, J., and Happe, T. (2008) *Eukaryot. Cell* **7**, 518–526
- Forestier, M., King, P., Zhang, L., Posewitz, M., Schwarzer, S., Happe, T., Ghirardi, M. L., and Seibert, M. (2003) *Eur. J. Biochem.* **270**, 2750–2758
- Happe, T., and Kaminski, A. (2002) *Eur. J. Biochem.* **269**, 1022–1032
- Happe, T., Mosler, B., and Naber, J. D. (1994) *Eur. J. Biochem.* **222**, 769–774
- Roessler, P. G., and Lien, S. (1984) *Plant Physiol.* **75**, 705–709
- Posewitz, M. C., King, P. W., Smolinski, S. L., Zhang, L., Seibert, M., and Ghirardi, M. L. (2004) *J. Biol. Chem.* **279**, 25711–25720
- Posewitz, M. C., King, P. W., Smolinski, S. L., Smith, R. D., Ginley, A. R., Ghirardi, M. L., and Seibert, M. (2005) *Biochem. Soc. Trans.* **33**, 102–104
- Posewitz, M. C., Mulder, D. W., and Peters, J. W. (2008) *Curr. Chem. Biol.* **2**, 178–199
- McGlynn, S. E., Ruebush, S. S., Naumov, A., Nagy, L. E., Dubini, A., King, P. W., Broderick, J. B., Posewitz, M. C., and Peters, J. W. (2007) *J. Biol. Inorg. Chem.* **12**, 443–447
- Bock, A., King, P. W., Blokesch, M., and Posewitz, M. C. (2006) *Adv. Microb. Physiol.* **51**, 1–71
- Harris, E. H. (1989) *The Chlamydomonas Sourcebook. A Comprehensive Guide to Biology and Laboratory Use*, pp. 780–785, Academic Press, San Diego
- Ghirardi, M., Togasaki, R., and Seibert, M. (1997) *Appl. Biochem. Biotech.* **63–5**, 141–151
- Livak, K. J., and Schmittgen, T. D. (2001) *Methods (San Diego)* **25**, 402–408
- Eberhard, S., Jain, M., Im, C. S., Pollock, S., Shrager, J., Lin, Y., Peek, A. S., and Grossman, A. R. (2006) *Curr. Genet.* **49**, 106–124
- Im, C. S., Zhang, Z., Shrager, J., Chang, C. W., and Grossman, A. R. (2003) *Photosynth. Res.* **75**, 111–125
- Li, Y., Horsman, M., Wu, N., Lan, C. Q., and Dubois-Calero, N. (2008) *Biotechnol. Prog.* **24**, 815–820
- Melis, A., Seibert, M., and Ghirardi, M. L. (2007) *Adv. Exp. Med. Biol.* **616**, 110–121
- Nagy, L. E., Meuser, J. E., Plummer, S., Seibert, M., Ghirardi, M. L., King, P. W., Ahmann, D., and Posewitz, M. C. (2007) *Biotechnol. Lett.* **29**, 421–430
- Ghirardi, M. L., King, P. W., Posewitz, M. C., Maness, P. C., Fedorov, A., Kim, K., Cohen, J., Schulten, K., and Seibert, M. (2005) *Biochem. Soc. Trans.* **33**, 70–72
- Quinn, J. M., Eriksson, M., Moseley, J. L., and Merchant, S. (2002) *Plant Physiol.* **128**, 463–471
- Moseley, J., Quinn, J., Eriksson, M., and Merchant, S. (2000) *EMBO J.* **19**, 2139–2151
- Rochaix, J. D. (2002) *FEBS Lett.* **529**, 34–38
- Melis, A., and Happe, T. (2001) *Plant Physiol.* **127**, 740–748
- Kruse, O., Rupprecht, J., Bader, K. P., Thomas-Hall, S., Schenk, P. M., Finazzi, G., and Hankamer, B. (2005) *J. Biol. Chem.* **280**, 34170–34177
- Harris, E. H. (2001) *Annu. Rev. Plant Physiol. Plant Mol. Biol.* **52**, 363–406
- Weaver, P. F., Lien, S., and Seibert, M. (1980) *Solar Energy* **24**, 3–45
- Seibert, M., King, P., Posewitz, M. C., Melis, A., and Ghirardi, M. L. (2008) *Bioenergy* (Wall, J., Demain, A., and Harwood, C., eds) pp. 273–291, American Society for Microbiology, Washington, D. C.
- Bologna, F. P., Andreo, C. S., and Drincovich, M. F. (2007) *J. Bacteriol.* **189**, 5937–5946
- Lee, S. J., Song, H., and Lee, S. Y. (2006) *Appl. Environ. Microbiol.* **72**, 1939–1948
- Stols, L., and Donnelly, M. I. (1997) *Appl. Environ. Microbiol.* **63**, 2695–2701
- Millard, C. S., Chao, Y. P., Liao, J. C., and Donnelly, M. I. (1996) *Appl. Environ. Microbiol.* **62**, 1808–1810
- Allmer, J., Naumann, B., Markert, C., Zhang, M., and Hippler, M. (2006) *Proteomics* **6**, 6207–6220
- Wagner, V., Gessner, G., Heiland, I., Kaminski, M., Hawat, S., Scheffler, K., and Mittag, M. (2006) *Eukaryot. Cell* **5**, 457–468
- Lemaire, S. D., Guillon, B., Le Marechal, P., Keryer, E., Miginiac-Maslow,

- M., and Decottignies, P. (2004) *Proc. Natl. Acad. Sci. U. S. A.* **101**, 7475–7480
49. Unden, G., and Bongaerts, J. (1997) *Biochim. Biophys. Acta* **1320**, 217–234
50. Richardson, D. J., Berks, B. C., Russell, D. A., Spiro, S., and Taylor, C. J. (2001) *Cell. Mol. Life Sci.* **58**, 165–178
51. Matias, P. M., Pereira, I. A., Soares, C. M., and Carrondo, M. A. (2005) *Prog. Biophys. Mol. Biol.* **89**, 292–329
52. Stoimenova, M., Igamberdiev, A. U., Gupta, K. J., and Hill, R. D. (2007) *Planta* **226**, 465–474
53. Ozawa, K., Meikari, T., Motohashi, K., Yoshida, M., and Akutsu, H. (2000) *J. Bacteriol.* **182**, 2200–2206
54. Bhandari, B., Naik, M. S., and Nicholas, D. J. D. (1984) *FEBS Lett.* **168**, 321–326
55. Arp, D. J., Chain, P. S., and Klotz, M. G. (2007) *Annu. Rev. Microbiol.* **61**, 503–528
56. Aparicio, P. J., Azuara, M. P., Ballesteros, A., and Fernandez, V. M. (1985) *Plant Physiol.* **78**, 803–806
57. Hodson, R. C., and Schiff, J. A. (1971) *Plant Physiol.* **47**, 296–299